HIV-1 Protease Mutations and Inhibitor Modifications Monitored on a Series of Complexes. Structural Basis for the Effect of the A71V Mutation on the Active Site†

Tereza Skálová,*,§ Jan Dohnálek,§ Jarmila Dušková,§ Hana Petroková,§ Martin Hradílek,‡ Milan Souček,‡ Jan Konvalinka,‡ and Jindřich Hašek§

Institute of Macromolecular Chemistry, Academy of Sciences of the Czech Republic, Heyrovského nám. 2, 162 06 Praha 6, Czech Republic, and Institute of Organic Chemistry and Biochemistry, Academy of Sciences of the Czech Republic, Flemingovo nám. 2, 166 10 Praha 6, Czech Republic

Received May 11, 2006

Two new X-ray structures of an HIV-1 protease mutant (A71V, V82T, I84V) in complex with inhibitors SE and SQ, pseudotetrapeptide inhibitors with an acyclic *S*-hydroxyethylamine isostere, were determined. Comparison of eight structures exploring the binding of four similar inhibitors—SE, SQ (*S*-hydroxyethylamine isostere), OE (ethyleneamine), and QF34 (hydroxyethylene)—to wild-type and A71V/V82T/I84V HIV-1 protease elucidates the principles of altered interaction with changing conditions. The A71V mutation, which is distant from the active site, causes changes in the structure of the enzyme detectable by the means of X-ray structure analysis, and a route of propagation of the effect toward the active site is proposed.

Introduction

Human immunodeficiency virus (HIV[a]) types 1 and 2 are retroviruses known as causal agents of acquired immunodeficiency syndrome (AIDS). HIV-1 protease, one of the targets of anti-AIDS drug design, is a 22 kDa dimeric aspartic protease that participates in maturation of the virus, cleaving the polyprotein precursor into functional viral proteins.

The HIV-1 protease structure has been known since 1989, when its first X-ray diffraction studies were published.[1−3] It is a homodimer, consisting of residues marked 1−99 (chain A) and 101−199 (chain B, Figure 1). Both monomers are related by pseudo-2-fold symmetry. The catalytic residues Asp25 and Asp125 lie at the bottom of the binding cavity covered by a pair of protease flaps (residues 44−55 and 144−155). Triads 25−26−27 and 125−126−127 form the base of the catalytic site, connected by hydrogen bonds in a so-called "fireman's grip"; it is the central rigid part of the dimer. In contrast, the protease flaps covering the binding cavity are flexible and their movement is thought to accompany ligand entry and binding. Two conformations of the protease flaps were repeatedly experimentally confirmed by X-ray crystallography. The complex with an active-site-bound ligand shows the flaps in a closed conformation connected by a hydrogen bond above the ligand. Nonliganded HIV-1 protease has flaps slightly risen in crystal structures (e.g., PDB code 1HHP).[4] Recently, a new conformation of HIV-1 protease in complex with metallacarborane inhibitors was observed in which the flaps adopt a wide open conformation.[5]

The binding modes of substrates and peptidomimetic inhibitors to HIV-1 protease were described generally in a number of reviews.[6,7] The scissile peptide bond or a reaction intermediate isostere binds to the catalytic residues Asp25 and Asp125, and the other ligand peptide bonds are bound to Gly27, Asp29, and Gly48 on one side of the chain and to Gly127, Asp129, and Gly148 in the opposite direction from the cleaved peptide bond. The ligand side chains are inserted into protease pockets S_1−S_4 and S_1'−S_4'.

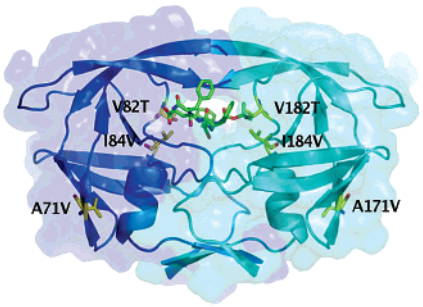

Figure 1. Overall view of HIV-1 protease dimer with inhibitor SE bound in the active site (I8−SE complex). Mutated residues are shown as sticks color-coded by atom types.

It is known that HIV-1 protease occurs in various mutant forms and that protease-targeted drug therapy leads to the selection of specific mutations in HIV-1 protease isolated from patients.[8] The mutated residues appear along the whole protease chain, both close to the active site and in distant parts of the molecule. It was found that the binding tunnel mutations decrease inhibitor and/or substrate binding affinity.[9] Some nonactive site mutations alone increase catalytic efficiency, and in combination with the active site mutations, they partially compensate for the reduction of catalytic efficiency caused by active site mutations.[9] Another study showed that some nonactive site mutations might also contribute significantly to destabilization of inhibitor binding.[10]

From a structural point of view, Munshi et al.[11] concluded that the 80s loop, the location of the most common active-site mutations, is highly flexible and adaptable. The conformation of the loop depends significantly on the bound inhibitor and can also be influenced by mutations in the loop. However, mutations are not necessary for conformational changes in the loop. To the best of our knowledge, a mechanism for the effect of the nonactive site mutations on inhibitor binding based on structural data has not yet been described.

Here, we present two new X-ray structures of mutant HIV-1 protease−inhibitor complexes. The mutations A71V, V82T, and

† The crystallographic data have been deposited in the Protein Data Bank under access codes 1ZJ7 (I8−SE) and 1ZLF (I8−SQ).

* To whom correspondence should be addressed. Telephone: +420 296 809 205. Fax: +420 296 809 410. E-mail: skalova@imc.cas.cz.

§ Institute of Macromolecular Chemistry.

‡ Institute of Organic Chemistry and Biochemistry.

[a] Abbreviations: HIV, human immunodeficiency virus; AIDS, acquired immunodeficiency syndrome; WT, wild type; Boc, *tert*-butyloxycarbonyl.

10.1021/jm0605583 CCC: $33.50
Published on Web 08/23/2006

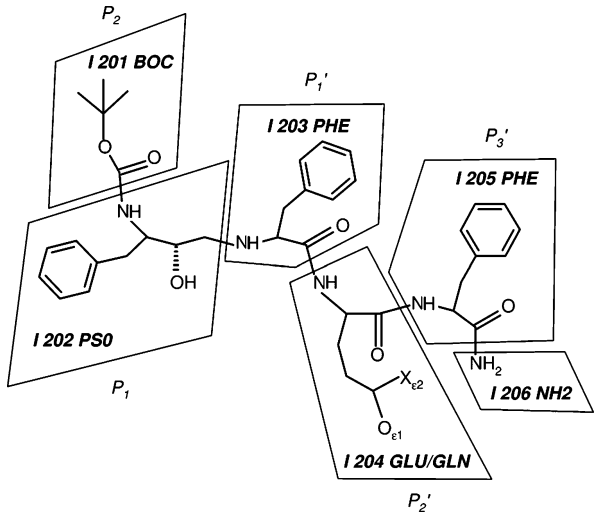

Figure 2. Scheme explaining the chemical structures of inhibitors SE and SQ with notation of positions P_2, P_1, P_1', P_2', P_3'. The inhibitors differ in the P_2' residue; $X_{\epsilon 2}$ is $O_{\epsilon 2}$ for the SE inhibitor and $N_{\epsilon 2}$ for the SQ inhibitor. Division of the inhibitors into residues I 201−I 206 corresponds to notation in the PDB records 1ZJ7 and 1ZLF.

Table 1. PDB Codes and Inhibition Constants of Two New HIV-1 Protease−Inhibitor Complexes, I8−SE and I8−SQ, and Six Other Previously Solved Structures[a]

	SE[b]		SQ[c]		OE[d]		QF34[e]	
	PDB	K_i, nM	PDB	K_i, nM	PDB	K_i, nM	PDB	K_i, nM
WT	1ZSR	0.15	1IIQ	33	1M0B	1.5	1IZH	0.02
I8	1ZJ7	86	1ZLF	1000	1LZQ	4.1	1IZI	0.26

[a] For details of K_i measurements, see refs 12, 16, and 17. [b] SE = Boc-Phe-ψ[*S*-CH(OH)CH_2NH]-Phe-Glu-Phe-NH_2. [c] SQ = Boc-Phe-ψ[*S*-CH(OH)-CH_2NH]-Phe-Gln-Phe-NH_2. [d] OE = Boc-Phe-ψ[CH_2CH_2NH]-Phe-Glu-Phe-NH_2. [e] QF34 = Boc-Phe-ψ[*S*-CH(OH)CH_2]-Phe-Gln-Phe-NH_2.

I84V (HIV-1 containing all three mutations is denoted as mutant I8) are selected in response to treatment by indinavir.[8] Residues 82 and 84 are active site residues; they form part of the above-mentioned 80s loop, which usually winds around the ligand side chains P_1 and P_1'. Residue 71 (valine in the BRU WT) is located ~16 Å from the active site in a β-sheet on the surface of the protease. The Val71 side chain is oriented toward the interior of the molecule.

The inhibitors studied are pseudotetrapeptides denoted as SE/SQ with chemical formula Boc-Phe-ψ[*S*-CH(OH)CH_2NH]-Phe-Glu/Gln-Phe-NH_2 (Figure 2).[12] The acronyms SE and SQ indicate the *S* configuration of the carbon in the isostere bearing the hydroxyl group and the type of the residue in the P_2' position (E/Q). Acronyms for complexes (e.g., WT−SQ) denote the protein type (wild-type, WT) and the inhibitor (SQ). Structures of complexes I8−SE and I8−SQ, newly determined within this study, are also compared with previously published structures WT−SE,[13] WT−SQ,[14] WT−OE,[15] I8−OE,[16] WT−QF34,[17] and I8−QF34.[17] These structures form a unique series of similar and potent inhibitors with published structural data (for PDB codes[18] and inhibition constants, see Table 1).

Results: Crystal Structures of I8−SE and I8−SQ Complexes

Protease Conformation. The overall view of SE inhibitor bound to mutated HIV-1 protease is shown in Figure 1. Both protease molecules in structures I8−SE and I8−SQ adopt the "closed" conformation typical of liganded complexes of HIV-1 protease, in which the flaps are closed and make contact with each other and with the inhibitor. The two protease dimers have nearly identical positions of corresponding C_α atoms (the rms deviation of all protease C_α positions is 0.2 Å), and the protein structure does not differ significantly from that of the majority of other complexes.

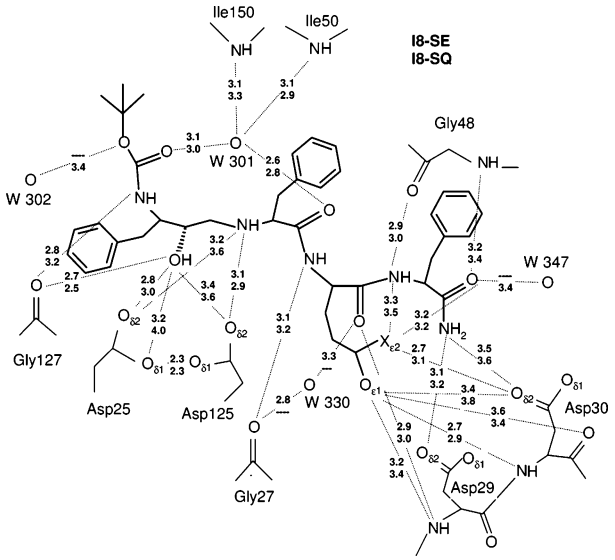

Figure 3. Hydrogen-bonding interactions between the SE/SQ inhibitor and HIV-1 protease mutant I8. The upper values correspond to the I8−SE complex, and the lower values correspond to the I8−SQ complex. All potential NH···O and OH···O hydrogen bonds up to a 3.6 Å donor−acceptor distance existing in at least one of the complexes are shown.

Alternative Conformations. Two possibilities for hydrogen-bonding interaction between flaps introduce alternative conformations in peptide bonds Ile50−Gly51 and Ile150−Gly151. Side chains of Phe53 and Phe153, which take part in crystal contacts, were also found in alternative conformations. Additionally, there are alternative conformations of side chains of Ile3, Gln7, Glu21, Glu34, Met46, Ile50, Val75, and Val84 (mutated residue) in the I8−SE structure and of residues Ile3, Trp42, Ile62, Ile103, Trp142, and Ile162 in the I8−SQ structure.

Inhibitor−Hydrogen Bonds. Both inhibitors bind to the protease binding pockets S_2, S_1, S_1', S_2', S_3' and form numerous hydrogen bonds along the inhibitor main chain and a hydrogen bond network along the hydrophilic side chain P_2'. All hydrogen bond donors and acceptors of the inhibitors are saturated (Figure 3). Both inhibitors' main chains bind to protease residues Asp25, Gly27, Gly48, Asp29, and Ile50 (mediated by a water molecule) and in this way follow the substrate binding scheme.[7,19]

I8−SE. The SE inhibitor in I8 HIV-1 protease forms 18 NH···O and OH···O hydrogen bonds (up to 3.6 Å, Figure 3) to the enzyme. Additionally, two water molecules mediate contacts between the inhibitor and the protease. There are two hydrogen bonds between the inhibitor and water molecule W 301 (which mediates connection to the protease flaps), and there is a hydrogen bond between the inhibitor and a buried water molecule W 330, which binds to Arg108 N_ϵ and Gly27 O.

The hydroxyl group of the peptide bond isostere forms hydrogen bonds to both $O_{\delta 1}$ and $O_{\delta 2}$ of Asp25 and to $O_{\delta 2}$ of Asp125. The isosteric amino group also forms hydrogen bonds to $O_{\delta 2}$ of Asp25 and Asp125. Many inhibitor−protease hydrogen bonds are concentrated in the region of the S_2' binding pocket, where hydrogen bonds exist between the inhibitor glutamic acid and protease residues Asp29 and Asp30.

I8−SQ. The SQ inhibitor in mutant HIV protease forms 16 NH···O and OH···O hydrogen bonds to the enzyme, and the binding scheme is similar to that of SE (Figure 3). Water molecule W 301 is bound similarly as in the I8−SE complex.

Table 2. HIV-1 Protease Residues with Close Contacts (up to 4.1 Å) with Inhibitors SE and SQ in Complexes I8−SE and I8−SQ[a]

S_2		S_1		S_1'		S_2'		S_3'	
SQ	SE	SQ	SE	SQ	SE	SQ	SE	SQ	SE
I50	I50	R8	R8	*D25*	*D25*	*G27*	*G27*	*D29*	*D29*
	G127	L23	L23	G27	G27	A28	A28	*D30*	*D30*
A128	A128	*D25*	*D25*	G49	G49	*D29*	*D29*	I47	I47
D129	D129		P81	I50	I50	*D30*	*D30*	*G48*	*G48*
D130	D130		T82	L123				G49	G49
V132	V132	*D125*	*D125*	*D125*	*D125*	I47	I47	F53	F53
I147	I147	*G127*	*G127*	I150					R108
G148	G148	A128	A128	P181	P181				P181
G149	G149	G149		T182	T182				
V184	V184	I150		V184	V184				

[a] The italicized protease residues form classical hydrogen bonds to the corresponding inhibitor residue.

Water W 302 (on the protease surface, bound to atoms N and $O_{\delta 2}$ of Asp129) forms a hydrogen bond to the ester oxygen of I 201 BOC of the inhibitor. W 347 is also localized on the protease surface (it binds to Asp30 $O_{\delta 2}$ and Lys45 N_{ζ}) and forms a hydrogen bond to the terminal amide group of the inhibitor. No water molecule analogous to the buried W 330 in the I8−SE complex was found in the I8−SQ complex.

The isostere binding to the catalytic aspartic acids is less tight than in the case of I8−SE, with longer distances between the hydroxyl and amine on one side and the carboxyls of Asp25 and Asp125 on the other.

Inhibitor−van der Waals and Other Weak Interactions. Existence of hydrogen bonds may not be the only critical factor in protein−ligand binding. To cover other possible types of interactions, all protease residues within 4.1 Å of the inhibitor are listed in Table 2. The largest contact differences between SE and SQ in this table are connected with the altered conformation of the P_1 phenyl ring (Figure 6) and the Ile150 side chain. Furthermore, the SQ P_1' phenyl ring is shifted by ~0.4 Å away from the center of the active site. This conformational shift propagates to the P_3' phenyl ring, which loosens close interaction with Pro181 in the I8−SQ complex.

Discussion: Structural Changes in Eight HIV-1 Protease−Inhibitor Complexes

To analyze the effects of HIV-1 protease mutations and of changes in the inhibitor chemistry, eight closely related X-ray structures, four with wild-type and four with the I8 mutant protease (Table 1), were compared.

1. Common Features and Differences. Conformational Strain. The eight X-ray structures were superimposed by the C and N terminal regions of their C_α traces (residues 1−11, 87−99, 101−111, and 187−199). This manner of superposition properly shows the differences around the active site and in flexible parts of the protease dimer. The rmsd values for the superimposed regions within pairs of studied complexes fluctuate around 0.3 Å.

The overall view of inhibitor binding in the eight complexes is shown in Figure 4, colored according to temperature factor (temperature *B* factor is proportional to the square of mean deviation of an atom from its determined position). The inhibitor atoms in the P_2, P_1', and P_2' positions consistently show the lowest *B* factors within the inhibitor. The P_1 position is the region of the highest *B* factors, and large structural differences in this region are therefore associated with a relatively poorly defined position of the P_1 side chain in most of these complexes. This probably results from conformational strain on the inhibitor when the P_1 side chain binds in the S_1 pocket because inhibitors with a peptide bond isostere longer than the peptide bond of

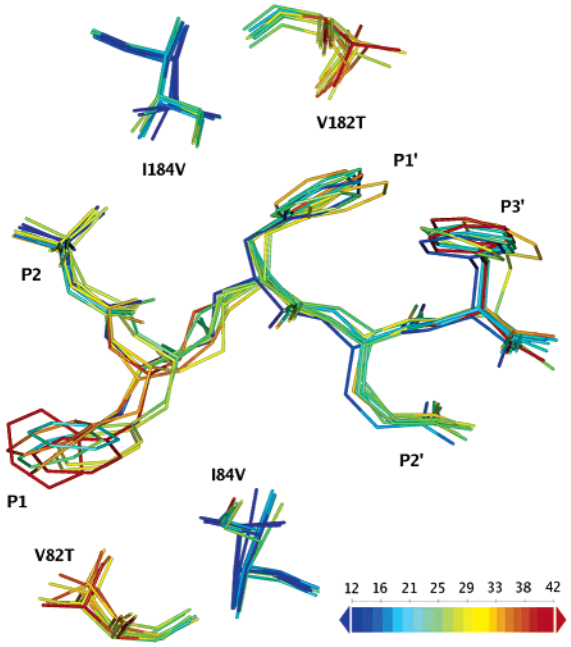

Figure 4. Overall comparison of SE, SQ, OE, and QF34 inhibitors binding to WT and I8 HIV-1 protease (superposition of eight X-ray structures). Atoms are colored by temperature *B* factors. Atoms of P_2, P_1', and P_2' residues have the most stable positions within the inhibitor, while P_1 is the most mobile. The figure also shows the positions of the mutated residues 82 (182) and 84 (184) and the relative difference of their *B* factors. Temperature factors of individual structures were shifted to obtain equal average nonsolvent *B* values (30 Å^2) in all structures.

natural substrates slightly displace the P_1 main chain and thus change demands on accommodation of the P_1 side chain in the S_1 pocket. Structure I8−SQ is distinct from the other SE, SQ, and OE complexes in placement of its P_1 residue (discussed later). Both QF34 complexes also show a unique position of P_1, which can be explained by the different length of its isostere.

A simple energetic analysis of eight protease−inhibitor complexes was performed to evaluate the importance of conformational strain in the studied complexes. The strain on inhibitor torsion angles was computed in InsightII[20] and compared for inhibitor conformation in the protease ($E_{\text{torsion,in}}$) and after its relaxation in an unbound state ($E_{\text{torsion,out}}$). Changes in the torsional strain for individual inhibitors ($\Delta E_{\text{torsion}} = E_{\text{torsion,in}} - E_{\text{torsion,out}}$) are presented in Figure 5. For all four inhibitors, there is higher torsional strain ($\Delta E_{\text{torsion}}$) in complex with the mutated protease than in complex with WT. A possible structural explanation of this behavior (mutation A71V) will be discussed later.

2. Changes in Inhibitor Isostere.

2.1. Isostere Binding to Catalytic Aspartates. In the SE and SQ complexes, the isostere is bound to catalytic aspartates by its hydroxy and amino groups, with the shortest hydrogen bonds between the hydroxyl and Asp25 $O_{\delta 2}$ and between the amine and Asp125 $O_{\delta 2}$ (Table 3). In the case of the OE inhibitor, which lacks a hydroxy group, the isostere amine binds to the catalytic aspartates in a similar way, with only a slightly shorter hydrogen bond to Asp125 $O_{\delta 2}$ than in the cases of inhibitors with a hydroxyethylamine moiety. QF34, which has a shorter isostere, places its hydroxy group more symmetrically with respect to the protease 2-fold symmetry and makes two short hydrogen bonds to both Asp25 $O_{\delta 2}$ and Asp125 $O_{\delta 2}$.

2.2. Isostere Conformation. The isostere conformation of inhibitors SE, SQ, and OE can be described by four torsion angles (Table 4). The isostere conformations of SE and SQ are similar in their complexes with the I8 mutant. The conformations

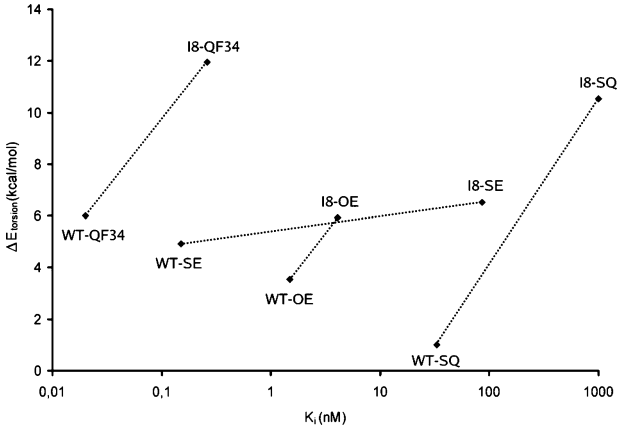

Figure 5. Relation between torsional strain $\Delta E_{torsion}$ and inhibition constants for eight WT and I8 HIV-1 protease complexes with inhibitors SE, SQ, OE, and QF34. Strain in torsion angles is greater in mutant I8 protease complexes than in the corresponding WT complexes. The energy values $\Delta E_{torsion}$ are differences in torsional energy of the inhibitor bound to the protease (without minimization) and torsional energy of the free inhibitor after relaxation (energy minimization).

Table 3. Lengths (Å) of Hydrogen-Bonding Interactions of Inhibitor Isosteres and the Catalytic Residues Asp25 and Asp125 and between Asp25 and Asp125 in Eight Complexes of WT and I8 HIV-1 Protease with Inhibitors SE, SQ, OE, and QF34

		SE	SQ	OE	QF34
WT	$OH_{isostere}\cdots Asp25\ O_{\delta 2}$	2.9	2.7		2.8
I8		2.8	3.0		2.8
WT	$OH_{isostere}\cdots Asp125\ O_{\delta 2}$	3.4			2.8
I8		3.4	3.6		2.7
WT	$NH_{isostere}\cdots Asp25\ O_{\delta 2}$	3.6	3.0		
I8		3.2	3.6	3.3	
WT	$NH_{isostere}\cdots Asp125\ O_{\delta 2}$	2.7	2.6	2.5	
I8		3.1	2.9	2.7	
WT	$Asp25\ O_{\delta 1}\cdots Asp125\ O_{\delta 1}$	2.7	2.7	2.5	2.6
I8		2.3	2.3	2.3	2.7

Table 4. Isostere "Main Chain" Torsion Angles Characterized by Division into Three Different Conformation Types[a]

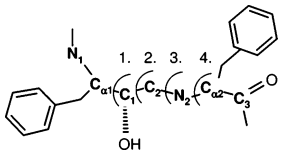

	WT−SE WT−SQ	I8−SE	I8−SQ WT−OE I8−OE
1. $N_1-C_{\alpha 1}-C_1-C_2$	*g*	*g*	*y*
2. $C_{\alpha 1}-C_1-C_2-N_2$	*t*	$-y$	$-y$
3. $C_1-C_2-N_2-C_{\alpha 2}$	$-y$	*t*	*t*
4. $C_2-N_2-C_{\alpha 2}-C_3$	*g*	*c*	*c*

[a] Approximate values of torsion angles are marked as follows: $c \approx 0°$, $\pm g \approx \pm 60°$, $\pm y \approx \pm 120°$, $t \approx 180°$.

are also similar in their WT complexes, which are distinct from those of the mutant complexes (Figure 6A). In the case of the OE inhibitor, conformation of the isostere is similar in both the WT and mutant complexes (Figure 6B). Conformation of the isostere of QF34 cannot be described by the same torsion angles as for SE, SQ, and OE; however, it is essentially the same in both the WT and I8 complexes (see the comparison with the SQ case in Figure 6C).

In the cases of SE, SQ, and OE (not QF34), the isostere is somewhat shifted from the aspartates toward the flaps in the mutant complexes compared to the wild-type ones (a 0.6 Å shift of I202 C of SQ between WT and I8 and 0.5 Å in SE and OE). This could be a result of the A71V mutation as discussed below.

3. Changes in P_2' Position. The WT and I8 complexes of SE and SQ differ by one hydrogen bond between the inhibitor's terminal NH_2 group and Asp29 $O_{\delta 2}$, which exists only in I8 complexes (Figure 7). Otherwise, the hydrogen-bonding scheme is similar in all four cases. It should be noted that hydrogen bonds in the S_2' pocket are stronger in WT−SQ than in WT−SE, and the inverse is observed in the I8 mutant complexes.

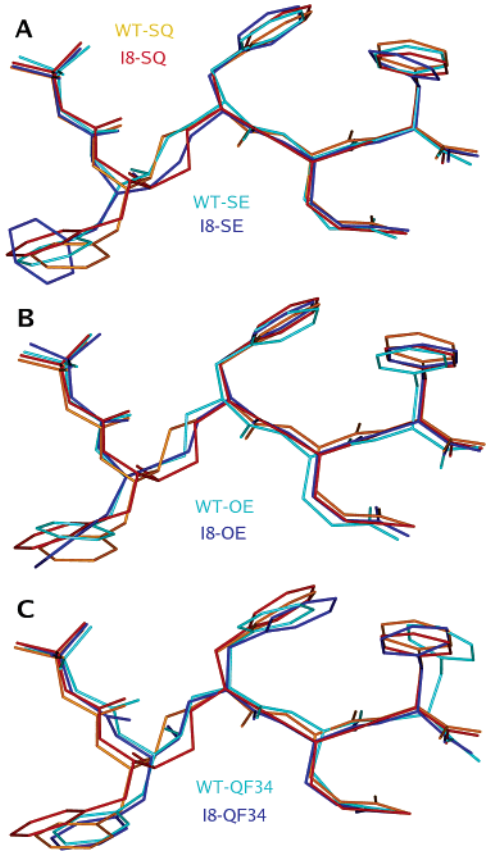

Figure 6. Comparison of the analyzed inhibitors based on superposition of protease−inhibitor complexes to illustrate the main differences in isostere conformation. WT−SQ (orange) and I8−SQ (red) are compared to (A) WT−SE (turquoise) and I8−SE (blue), (B) WT−OE (turquoise) and I8−OE (blue), and (C) WT−QF34 (turquoise) and I8-QF34 (blue).

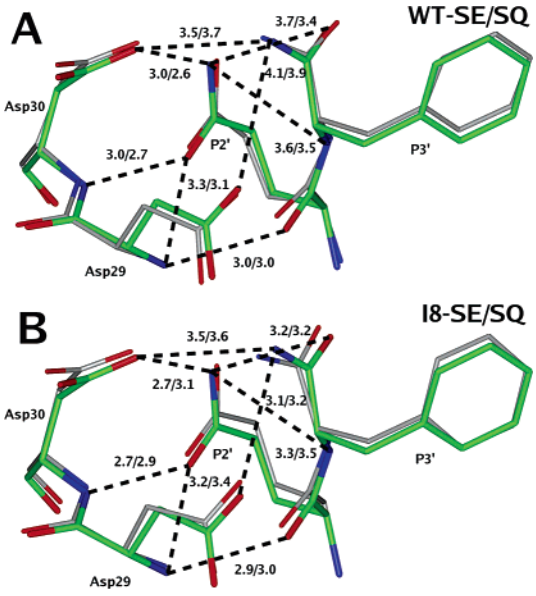

Figure 7. Binding scheme of SE (gray) and SQ (green) to the S_2' subsite of WT and I8 HIV-1 protease. Notice that both inter- and intramolecular contacts determine the network of hydrogen bonds at the S_2' subsite.

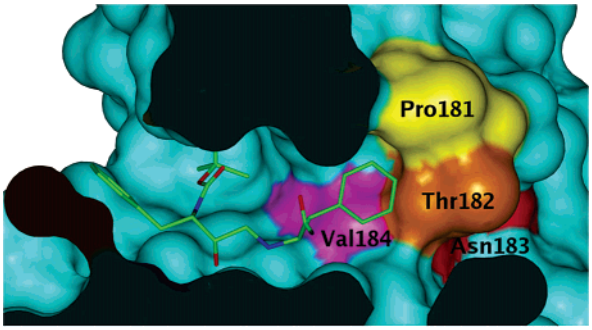

Figure 8. P_1' binding site of SE bound to I8 HIV-1 protease. The inhibitor is shown as a sticks model and the protease as a section of its solvent accessible surface with distinctly colored residues of the loop 181−184, including mutated residues V182T and I184V. This is the region of the closest contacts between the discussed HIV-1 protease mutation sites and the inhibitor.

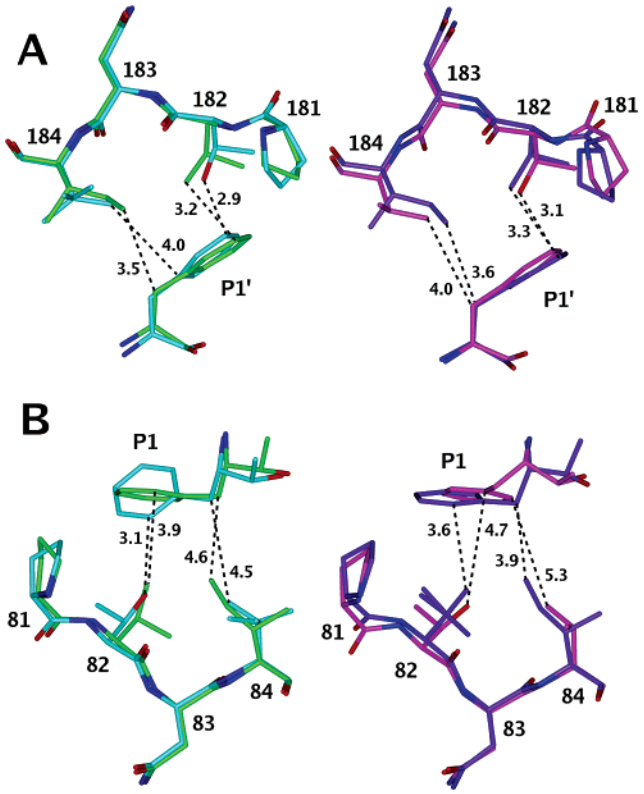

Figure 9. Close contacts between the inhibitor phenyl rings in the (A) P_1' and (B) P_1 positions and mutated residues V82T and I84V in the complexes WT−SE (green), I8−SE (turquoise), WT−SQ (violet), and I8−SQ (pink). Residues Val84 and Val184 in I8−SE and Val82 in WT−SQ occur in two alternative conformations.

4. Effects of HIV-1 Protease Mutations.

4.1. Effects of Mutations V82T and I84V. Residues 81−84 (181−184) form a wall of the ligand binding tunnel in the binding pocket S_1 (S_1') (Figure 8). As shown in Figure 4, residues 82 and 84 differ considerably in temperature factors, 82 having higher mobility than 84. For inhibitors SE, SQ, and OE, contacts with the binding pocket S_1' are tighter than with S_1. In QF34, the situation in both pockets is more or less equal. A comparison of protease mutation sites in complexes WT−SE, WT−SQ, I8−SE, and I8−SQ is shown in Figure 9.

4.1.1. Binding Site S_1. The inhibitors differ in the mode of insertion of the side chain into the pocket (Figure 9). The case of I8−SQ is the most outstanding one, in which the P_1 side chain enters the S_1 pocket from a different direction when compared to the other complexes. This can be illustrated by the distance between the I 202 C_α positions in I8−SE and I8−SQ of 1.0 Å and between the C_β atoms of 2.0 Å. The inhibitor conformations also differ in torsion of the P_1 phenyl ring. The way in which the phenylalanine side chain is situated and the shape of the S_1 binding pocket are tightly connected. Differences in the shape of the binding pocket are mainly caused by conformational changes of residues Pro81 and Val/Thr 82. In the case of I8−SE, the ring is inserted in a parallel position between the Thr82 side chain and the ring of Pro81. In the other three cases the ring is roughly parallel to the 81−82 main chain. In the I8−SQ complex, Thr82 does not interact with P_1 because of the different torsion of the P_1 phenyl ring.

As follows from the previous discussion, in the cases of inhibitors with longer isosteres, differences in inhibitor conformation near the S_1 binding pocket are not necessarily predominantly caused by mutations. The different binding of I8−SQ in this area is the main observable structural difference within the group of WT and I8 complexes with SE, SQ, and OE, and it appears for the complex with the highest K_i. The higher value of K_i of I8−SQ in comparison with I8−SE may be a result of different intramolecular interactions within the inhibitors in their bound and solvated states.

4.1.2. Binding Site S_1'. Observed changes in the S_1' binding site are more systematic than in S_1 and can be explained as effects of protease mutations.

There appears to be a tighter contact between residue 182 and the inhibitor in the mutant complexes than in the WT complexes, and an interaction forms between the Thr182 hydroxy group and the P_1' phenyl ring. Thr182 has its $O_{\gamma 1}$ placed above the P_1' phenyl ring with the closest contact of 2.9 Å to I 203 $C_{\epsilon 2}$ (I8−SE) or 3.1 Å to I 203 $C_{\epsilon 2}$ and C_ς (I8−SQ).

Residue Ile/Val 184 is also in tight contact with P_1' phenylalanine (the closest contacts are of C···C type, ∼4.0 Å). In the cases of mutant protease complexes, the presence of valine in position 184 decreases the number of van der Waals contacts between the enzyme and the P_1' phenyl ring. This both weakens the overall protease−inhibitor interactions[16] and at the same time gives more freedom to the P_1' phenyl ring and enables its relaxation in χ_2 torsion. The small change in the χ_2 torsion angle of the P_1' phenyl ring is connected with a change in Pro181 conformation (it is different in WT−SE/SQ and I8−SE/SQ complexes) and also with the position of the P_3' phenyl ring interacting directly with the P_1' ring. The consequent shift of the P_3' side chain is in concert with the movement of the Asp29 side chain. This seemingly insignificant change in Asp29 conformation results in a new hydrogen bond between the inhibitor terminal NH_2 group and Asp29 $O_{\delta 2}$ in the I8 complexes (compared to WT).

4.2. Effects of the A71V Mutation. Superposition of the protease chains only by their rigid N and C terminal regions (defined above) enables a more detailed description of changes in other parts of the protease−inhibitor complexes. The mutation of Ala71 to valine requires more space to accommodate valine's bulkier side chain, which is oriented toward the enzyme interior. These requirements are met by a shift of the 70−71 main chain away from the loop encompassed by residues 92−93. The protease region 24−71 includes a four-stranded β-sheet, which partly behaves like a rigid ensemble. On the basis of the reported structures, it seems that the β-sheet movement can be propagated as far as the catalytic residue Asp25 and can change the shape of the ligand binding tunnel. The propagation of the shift from the mutation site to the catalytic center and a scheme of significant hydrogen bonds between β-strands (connecting residues 71···64, 65···14, 13···20) are shown in Figure 10.

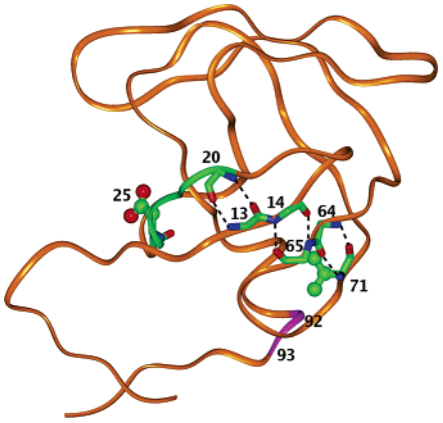

Figure 10. Route of propagation of the shift of the HIV-1 protease β-sheet caused by the mutation A71V. For clarity, only one of the two monomers of HIV-1 protease is displayed schematically by a ribbon (orange). Residues 92−93, typically found in different distances from the 70−71 main chain in the "Ala71" and "Val71" structures, are colored purple. The region of the β-sheet connecting Val71 with Asp25 is represented by sticks or balls-and-sticks and color-coded by atom type (carbon is green, nitrogen is blue, oxygen is red) with dashed lines indicating hydrogen bonds.

In the cases of the SE and SQ inhibitors, the I8 protease complexes have a distance between the 92−93 and 70−71 chains longer by ∼0.5 Å than in WT complexes. In both cases, the whole β-sheet is somewhat shifted and rotated in comparison to the WT complexes. The shortening of the hydrogen bond between Asp25 and Asp125 in the I8 complexes (Table 3) is likely to be connected with this β-sheet movement caused by the A71V mutation.

Similar effects appear in the WT−OE and I8−OE complexes. In the QF34 structures, the shift of the β-sheet is also apparent; however, the distortion of the 19−25 chain relaxes along the peptide backbone and the Asp25−Asp125 hydrogen bond distance is similar in the WT and I8 complexes.

The change in the active site of the SE and SQ complexes (formation of low barrier hydrogen bond between the catalytic aspartates)[21] is in agreement with the "higher" position of the SE and SQ isosteres in the protease binding tunnel. Moreover, the increased conformational strain found computationally in the mutant protease complexes with the inhibitors SE, SQ, OE, and QF34 could be in part understood as a consequence of the above-described changes within the active site, all being reasons for higher K_i values in the I8−SE/SQ complexes.

To generalize conclusions on the influence of the A71V mutation on inhibitor binding, a PDB search was performed. Apart from the discussed set of structures, only four other liganded HIV-1 protease complexes with closed flaps and with the A71V mutation were found: 1HSH, 1C6X, 1C6Y, and 1C6Z. This number is not sufficient for generalized conclusions. However, HIV-2 protease contains Val71 in its wild-type sequence (ROD isolate[22]), and so at least some conclusions can be drawn regarding the presence of valine in position 71 if these structures are also included in the comparison set. Within the test set of approximately 30 HIV-1 protease structures with Ala71 and 30 HIV-1 and HIV-2 protease structures with Val71, it was found that the distances between chains 70−71 and 92−93 in the "Val71" subset are detectably larger, on average by ∼1 Å. The shift of the other protease chains caused by the A71V mutation is not generally detectable farther toward the catalytic residues, and the hydrogen bond distance Asp25 $O_{\delta1}$···Asp125 $O_{\delta1}$ is statistically the same ($\langle d \rangle$ = 2.8 Å) in the "Val71" and "Ala71" subsets.

Conclusion

The comparison of eight HIV protease−inhibitor structures leads to the following conclusions. These types of inhibitors form a saturated network of hydrogen bonds to both WT and I8 protease. The complex with the highest K_i value, I8−SQ, has the most distinct binding mode within the set, mainly in the region of P_1. The subnanomolar K_i of QF34 for both the WT and I8 complexes in comparison to the SE and SQ inhibitors is most likely a result of its shorter isostere, which enables a better fit of P_1 and P_1' side chains in the protease binding pockets.

Structural comparison of differences in the P_2' side chains (Glu/Gln) of SE and SQ showed basically the same type of binding in both cases. Even if it was observed that the order of the strength of interaction between P_2' and S_2' (measured by hydrogen bond distances) changes from the WT (SQ stronger than SE) to the I8 (SE stronger than SQ) complexes, the overall effect of this simple chemical change on the inhibitor affinity is very likely connected with intramolecular interactions between P_2' and the rest of the inhibitor in solution and in the bound state.[23]

For the studied series of inhibitors, conformational strain in inhibitor bound to the protease proved to be a relevant parameter for correlation of structural results and measured inhibitor affinities with respect to the changes observed when comparing the wild type to the triple mutant A71V/V82T/I84V. Torsional strain is only one selected part of Gibbs energy, and therefore, full quantitative correspondence with K_i values cannot be expected (the SE WT−I8 energy difference in Figure 5 shows a slope distinct from those of the other cases).

It follows from this detailed analysis of the series of closely related inhibitors that the measured affinity differences of the extreme cases (the highest and the lowest K_i values) are clearly correlated with the observed changes in the structures (I8−SQ and QF34 complexes). Moreover, because the whole set of carefully determined complexes with relatively small individual changes is available, it can successfully explain inhibition properties of these compounds toward WT and mutant forms of the viral protease via additional computational analysis (e.g., through the conformational strain analysis) in correlation with experimental data.

It was postulated in the past that nonactive site mutations of HIV-1 protease can affect the stability of a bound inhibitor via long-range interactions.[7,10] Here, for the first time we present structural experimental data that lead to the conclusion that the A71V mutation leads to a significant deformation of the protease dimer, eventually resulting in changes within the active site of the enzyme.

Experimental Section

Expression and purification of HIV-1 protease mutant I8 (A71V, V82T, I84V; mutations with respect to the BRU isolate sequence) were described in ref 16. Synthesis of inhibitors SQ and SE was described in refs 14 and 24.

Crystallization and Data Collection (I8−SE, I8−SQ). The crystals were prepared using the hanging drop vapor diffusion technique at 298 K. The reservoir solution contained 0.1 M sodium citrate, 0.5 M sodium chloride, and 10% (v/v) glycerol, pH 4.4. The diffraction data for both complexes were collected at ESRF in Grenoble, beamline ID14-1 at 100 K on a MarCCD detector, with a wavelength of 0.934 Å and an oscillation angle of 1°. Data and structure statistics for the I8−SE and I8−SQ complexes are shown in Table 5.

Table 5. Data and Structural Statistics for I8−SE and I8−SQ Protease−Inhibitor Complexes[a]

HIV-1 protease−inhibitor complex	I8−SE	I8−SQ
HIV-1 protease mutation sites	A71V, V82T, I84V	A71V, V82T, I84V
PDB code	1ZJ7	1ZLF
X-ray source	ESRF ID14-1	ESRF ID14-1
resolution range (Å)	20.0−1.93 (2.02−1.93)	33.0−2.3 (2.38−2.30)
space group	$P6_122$	$P6_1$
unit cell parameters	$a = b = 62.86$ Å	$a = b = 62.78$ Å
	$c = 83.25$ Å	$c = 83.41$ Å
	$\alpha = \beta = 90°$	$\alpha = \beta = 90°$
	$\gamma = 120°$	$\gamma = 120°$
R_{merge}	0.048 (0.434)	0.049 (0.261)
data completeness (%)	87.6 (85.4)	90.8 (99.8)
no. of unique reflections	6784 (627)	7595 (831)
refinement program	CNS	CNS
no. of water molecules	67	60
average *B* factor (Å^2)	33.7	35.0
R	0.229 (0.357)	0.207 (0.295)
R_{free}	0.299 (0.371)	0.288 (0.379)
rmsd bond lengths from ideal (Å)	0.012	0.012
rmsd angles from ideal (deg)	1.7	1.7

[a] Values for the highest resolution shell are given in parentheses.

Data Processing, Structure Solution, and Refinement (I8−SE). The crystal belongs to the hexagonal $P6_122$ space group, with unit-cell parameters $a = b = 62.86$ Å, $c = 83.25$ Å, $\alpha = \beta = 90°$, and $\gamma = 120°$. The data were processed in a 20.0−1.93 Å resolution range with $R_{merge} = 0.048$.

Structure refinement was performed in CNS[25] using the R_{free} statistics on 5% of reflections. The final *R* factors are $R_{overall} = 0.229$ and $R_{free} = 0.299$. A total of 94% of residues lie in the most favored regions of the Ramachandran plot, and 4% lie in additionally allowed regions. One (Cys67) lies in the generously allowed region. The average coordinate error estimated from the Luzatti plot is 0.3 Å. The coordinates and structure factors of the I8−SE complex were deposited in the RCSB Protein Data Bank under accession codes 1ZJ7 and r1ZJ7sf. The PDB record contains one protease chain; the second chain of the dimer can be generated by symmetry operations. Symmetry operations will also generate the alternative orientation of the inhibitor SE.

Data Processing, Structure Solution, and Refinement (I8−SQ). The crystal belongs to the hexagonal $P6_1$ space group, with unit cell parameters $a = b = 62.78$ Å, $c = 83.41$ Å, $\alpha = \beta = 90°$, and $\gamma = 120°$. The data were processed in the resolution range 33.0−2.3 Å with $R_{merge} = 0.049$.

Structure refinement was performed in CNS[25] using the R_{free} statistics on 6.5% of reflections. The final *R* factors are $R_{overall} = 0.207$ and $R_{free} = 0.288$. A total of 95% of residues lie in the most favored regions of the Ramachandran plot and 5% in additionally allowed regions. The coordination error estimated from the Luzatti plot is 0.3 Å. The coordinates and structure factors of the I8−SQ complex were deposited in the RCSB Protein Data Bank under accession codes 1ZLF and r1ZLFsf. The PDB record corresponds to a biological unit, the HIV-1 protease dimer with the inhibitor in two alternative conformations related by the noncrystallographic 2-fold symmetry of the protease.

Computation of Torsional Strain in Inhibitors. The strain values $\Delta E_{torsion}$ were calculated by $\Delta E_{torsion} = E_{torsion,in} - E_{torsion,out}$, where $E_{torsion,in}$ is the torsional energy of the inhibitor when it is bound to HIV-1 protease and $E_{torsion,out}$ is the torsional energy of the free inhibitor after its energy minimization. $E_{torsion,in}$ and $E_{torsion,out}$ were computed in DISCOVER, InsightII.[20] The first conformation of the inhibitor in the corresponding PDB record was taken as the initial state of minimization with hydrogen atoms added in InsightII and force field CFF91. Energy was minimized by a combination of the steepest descent and conjugate gradient methods.

The graphics were prepared using PYMOL[26] (Figure 1) and InsightII[20] (Figures 4, 6−10).

Acknowledgment. This work was funded by the Grant Agency of the Academy of Sciences of the Czech Republic (Projects KJB4050312 and A4050811) and by the Ministry of Education, Youth and Sports of the Czech Republic under support of R&D (Project 1K05008). The authors thank the staff of ESRF in Grenoble, beamline ID14-1.

References

(1) Wlodawer, A.; Miller, A.; Jaskólski, M.; Sathyanarayana, B. K.; Baldwin, E.; Weber, I.; Selk, L. M.; Clawson, L.; Schneider, J.; Kent, S. B. H. Conserved folding in retroviral proteases: crystal structure of a synthetic HIV-1 protease. *Science* **1989**, *245*, 616−621.

(2) Miller, M.; Schneider, J.; Sathyanarayana, B. K.; Toth, M. V.; Marshall, G. R.; Clawson, L.; Selk, L.; Kent, S. B. H.; Wlodawer, A. Structure of complex of synthetic HIV-1 protease with a substrate-based inhibitor at 2.3-Å resolution. *Science* **1989**, *246*, 1149−1152.

(3) Lapatto, R.; Blundell, T.; Hemmings, A.; Overington, J.; Wilderspin, A.; Wood, S.; Merson, J. R.; Whittle, P. J.; Danley, D. E.; Geoghegan, K. F.; Hawrylik, S. J.; Lee, S. E.; Scheld, K. G.; Hobart, P. M. X-ray analysis of HIV-1 proteinase at 2.7 Å resolution confirms structural homology among retroviral enzymes. *Nature* **1989**, *342*, 299−302.

(4) Spinelli, S.; Liu, Q. Z.; Alzari, P. M.; Hirel, P. H.; Poljak, R. J. The three-dimensional structure of the aspartyl protease from the HIV-1 isolate Bru. *Biochimie* **1991**, *73*, 1391−1396.

(5) Cigler, P.; Kozisek, M.; Rezacova, P.; Brynda, J.; Otwinowski, Z.; Pokorna, J.; Plesek, J.; Gruner, B.; Doleckova-Maresova, L.; Masa, M.; Sedlacek, J.; Bodem, J.; Krausslich, H. G.; Kral, V.; Konvalinka, J. From nonpeptide toward noncarbon protease inhibitors: Metallacarboranes as specific and potent inhibitors of HIV protease. *Proc. Natl. Acad. Sci. U.S.A.* **2005**, *102* (43), 15394−15399.

(6) Babine, R. E.; Bender, S. L. Molecular recognition of protein−ligand complexes: applications to drug design. *Chem. Rev.* **1997**, *97*, 1359−1472.

(7) Wlodawer, A.; Vondrasek, J. Inhibitors of HIV-1 protease: A major success of structure-assisted drug design. *Annu. Rev. Biophys. Biomol. Struct.* **1998**, *27*, 249−284.

(8) Rhee, S. Y.; Fessel, W. J.; Zolopa, A. R.; Hurley, L.; Liu, T.; Taylor, J.; Nguyen, D. P.; Slome, S.; Klein, D.; Horberg, M.; Flamm, J.; Follansbee, S.; Schapiro, J. M.; Shafer, R. W. *J. Infect. Dis.* **2005**, *192*, 456−465; HIV drug resistance database, http://hivdb.stanford-.edu/.

(9) Schock, H. B.; Garsky, V. M.; Kuo, L. C. Mutational anatomy of an HIV-1 protease variant conferring cross-resistance to protease inhibitors in clinical trials. Compensatory modulations of binding and activity. *J. Biol. Chem.* **1996**, *271*, 31957−31963.

(10) Olsen, D. B.; Stahlhut, M. W.; Rutkowski, C. A.; Schock, H. B.; vanOlden, A. L.; Kuo, L. C. Non-active site changes elicit broad-based cross-resistance of the HIV-1 protease to inhibitors. *J. Biol. Chem.* **1999**, *274*, 23699−23701.

(11) Munshi, S.; Chen, Z. G.; Yan, Y. W.; Li, Y.; Olsen, D. B.; Schock, H. B.; Galvin, B. B.; Dorsey, B.; Kuo, L. C. An alternate binding site for the P1−P3 group of a class of potent HIV-1 protease inhibitors as a result of concerted structural change in the 80s loop of the protease. *Acta Crystallogr., Sect. D: Biol. Crystallogr.* **2000**, *56*, 381−388.

(12) Konvalinka, J.; Litera, J.; Weber, J.; Vondrášek, J.; Hradílek, M.; Souček, M.; Pichová, I.; Majer, P.; Štrop, P.; Sedláček, J.; Heuser, A. M.; Kottler, H.; Kräusslich, H. G. Configurations of diastereomeric hydroxyethylene isosteres strongly affect biological activities of a series of specific inhibitors of human-immunodeficiency-virus protease. *Eur. J. Biochem.* **1997**, *250*, 559−566.
(13) Dušková, J.; Dohnálek, J.; Skálová, T.; Petroková, H.; Hradílek, M.; Konvalinka, J.; Souček, M.; Brynda, J.; Fábry, M.; Sedláček, J.; Hašek, J. On the role of *R*-configuration of the reaction intermediate isostere in HIV-1 protease inhibitor binding; X-ray structure at 2.0 Å resolution. *Acta Crystallogr., Sect. D: Biol. Crystallogr.* **2006**, *62*, 489−497.
(14) Dohnalek, J.; Hasek, J.; Duskova, J.; Petrokova, H.; Hradilek, M.; Soucek, M.; Konvalinka, J.; Brynda, J.; Sedlacek, J.; Fabry, M. Hydroxyethylamine isostere of an HIV-1 protease inhibitor prefers its amine to the hydroxy group in binding to catalytic aspartates. A synchrotron study of HIV-1 protease in complex with a peptidomimetic inhibitor. *J. Med. Chem.* **2002**, *45*, 1432−1438.
(15) Petrokova, H.; Duskova, J.; Dohnalek, J.; Skalova, T.; Vondrackova-Buchtelova, E.; Soucek, M.; Konvalinka, J.; Brynda, J.; Fabry, M.; Sedlacek, J.; Hasek, J. Role of hydroxyl group and *R*/*S* configuration of isostere in binding properties of HIV-1 protease inhibitors. *Eur. J. Biochem.* **2004**, *271*, 4451−4461.
(16) Skalova, T.; Hasek, J.; Dohnalek, J.; Petrokova, H.; Buchtelova, E.; Duskova, J.; Soucek, M.; Majer, P.; Uhlikova, T.; Konvalinka, J. An ethylenamine inhibitor binds tightly to both wild type and mutant HIV-1 proteases. Structure and energy study. *J. Med. Chem.* **2003**, *46*, 1636−1644.
(17) Weber, J.; Mesters, J. R.; Lepsik, M.; Prejdova, J.; Svec, M.; Sponarova, J.; Mlcochova, P.; Skalicka, K.; Strisovsky, K.; Uhlikova, T.; Soucek, M.; Machala, L.; Stankova, M.; Vondrasek, J.; Klimkait, T.; Kraeusslich, H. G.; Hilgenfeld, R.; Konvalinka, J. Unusual binding mode of an HIV-1 protease inhibitor explains its potency against multi-drug-resistant virus strains. *J. Mol. Biol.* **2002**, *324*, 739−754.
(18) Berman, H. M.; Westbrook, J.; Feng, Z.; Gilliland, G.; Bhat, T. N.; Weissig, H.; Shindyalov, I. N.; Bourne, P. E. The Protein Data Bank. *Nucleic Acids Res.* **2000**, *28*, 235−242.
(19) Babine, R. E.; Bender, S. L. Molecular recognition of protein−ligand complexes: Applications to drug design. *Chem. Rev.* **1997**, *97*, 1359−1472.
(20) *InsightII*; Molecular Simulations, Inc.: San Diego, CA, 2000.
(21) Cleland, W. W.; Perry, A. F.; Gerlt, J. A. The low barrier hydrogen bond in enzymatic catalysis. *J. Biol. Chem.* **1998**, *273*, 25529−25532.
(22) Priestle, J. P.; Fässler, A.; Rosel, J.; Tinelnot-Blomley, M.; Strop, P.; Grütter, M. G. Comparative analysis of the X-ray structures of HIV-1 and HIV-2 proteases in complex with CGP 53820, a novel pseudosymmetric inhibitor. *Structure* **1995**, *15*, 381−389.
(23) Skalova, T. HIV-1 Protease and Its Interaction with Inhibitors. Ph.D. Thesis, Faculty of Mathematics and Physics, Charles University, Prague, Czech Republic, 2003.
(24) Dohnalek, J.; Hasek, J.; Duskova, J.; Petrokova, H.; Hradilek, M.; Soucek, M.; Konvalinka, J.; Brynda, J.; Sedlacek, J.; Fabry, M. A distinct binding mode of a hydroxyethylamine isostere inhibitor of HIV-1 protease. *Acta Crystallogr., Sect. D: Biol. Crystallogr.* **2001**, *57*, 472−476.
(25) Brunger, A. T.; Adams, P. D.; Clore, G. M.; DeLano, W. L.; Gros, P.; Grosse-Kunstleve, R. W.; Jiang, J. S.; Kuszewski, J.; Nilges, M.; Pannu, N. S.; et al. Crystallography & NMR system: A new software suite for macromolecular structure determination. *Acta Crystallogr., Sect. D: Biol. Crystallogr.* **1998**, *54*, 905−921.
(26) DeLano, W. L. The PyMOL Molecular Graphics System (2002). http://www.pymol.org.

JM0605583